IMECE2020-24189

REVERSE ELECTROWETTING-ON-DIELECTRIC ENERGY HARVESTING INTEGRATED WITH CHARGE AMPLIFIER AND RECTIFIER FOR SELF-POWERED MOTION SENSORS

Pashupati R. Adhikari
University of North Texas
Department of Mechanical and Energy Engineering
Denton, TX 76207

Nishat T. Tasneem, Dipon K. Biswas
University of North Texas
Department of Electrical Engineering
Denton, TX 76207

Russell C. Reid
Dixie State University
Department of Engineering
St. George, UT 84770

Ifana Mahbub
University of North Texas
Department of Electrical Engineering
Denton, TX 76207

ABSTRACT

This paper presents a reverse electrowetting-on-dielectric (REWOD) energy harvester integrated with rectifier, boost converter, and charge amplifier that is, without bias voltage, capable of powering wearable sensors for monitoring human health in real-time. REWOD has been demonstrated to effectively generate electrical current at a low frequency range (<3 Hz), which is the frequency range for various human activities such as walking, running, etc. However, the current generated from the REWOD without external bias source is insufficient to power such motion sensors. In this work, to eventually implement a fully self-powered motion sensor, we demonstrate a novel bias-free REWOD AC generation and then rectify, boost, and amplify the signal using commercial components. The unconditioned REWOD output of 95-240 mV AC is generated using a 50 µL droplet of 0.5M NaCl electrolyte and 2.5 mm of electrode displacement from an oscillation frequency range of 1-3 Hz. A seven-stage rectifier using Schottky diodes having a forward voltage drop of 135-240 mV and a forward current of 1 mA converts the generated AC signal to DC voltage. ~3 V DC is measured at the boost converter output, proving the system could function as a self-powered motion sensor. Additionally, a linear relationship of output DC voltage with respect to frequency and displacement demonstrates the potential of this REWOD energy harvester to function as a self-powered wearable motion sensor.

Keywords: Reverse electrowetting, Charge amplifier, DC-DC converter, Self-powered motion sensor

NOMENCLATURE

C	Capacitance
ε_o	Vacuum permittivity
ε_r	Relative permittivity of dielectric material
A	Electrode-electrolyte interfacial area
d	Dielectric layer thickness
C_{in}	Input capacitance
V_{in}	Input voltage
V_{out}	Output voltage
V_{P-P}	Peak-to-peak voltage
I_{rect}	Rectifier output current
V_{rect}	Rectifier output voltage
R	Resistance
L	Inductance
R_f	Gain Resistance
C_f	Feedback capacitance

1. INTRODUCTION

Portable health monitoring and motion tracking devices have remarkably emerged over the last few years as a primary source of continuous human health monitoring in real-time during daily life activities such as walking, running, etc. [1]. Typically, these devices are powered by an external power supply such as batteries. Although significant progress has been made in increasing the capacity of the batteries and reducing the power consumption of the devices, these systems still need rigid lithium-ion batteries with frequent replacement or charging process, which greatly limits their application and brings inconvenience [2]. The fundamental approach to eliminate this

issue is to integrate an energy harvester within the device itself and self-power it without requiring any external power source. Many energy harvesting technologies have emerged over the years such as piezoelectric, electromagnetic, triboelectric nanogenerator (TENG), and vibration-based energy harvesting that have been well established [3-6]. Among these energy harvesting technologies, TENG has been shown to efficiently generate power at low-frequency range; however, the underlying principle by which it operates (repeated contact between oppositely charged surfaces) significantly limits its long-term performance [7]. Other energy harvesting techniques have certain limitations, particularly in applications where the input frequency is at a lower range (< 5 Hz). Additionally, these energy harvesting techniques require resonance of solid structures to operate, which is typically over 50 Hz, making them quite unsuitable for harvesting energy from human motion-related activities.

Owing to the aforementioned limitations, energy harvesting based on reverse electrowetting-on-dielectric (REWOD) has been developed within the last decade [8], particularly due to its advantageous operation at lower frequencies without friction and not requiring resonance frequency. REWOD is opposite to electrowetting-on-dielectric (EWOD) in which an electric field applied to an electrolyte modifies the effective surface tension and produces electrolyte movement [9]. In REWOD, applied mechanical modulation changes electrolyte displacement and thereby changes the electrode-electrolyte interfacial area, generating alternating current.

Figure 1 illustrates an example of the REWOD configuration wherein the top electrode is coated with a metal layer that acts as a current collector. The bottom electrode is first
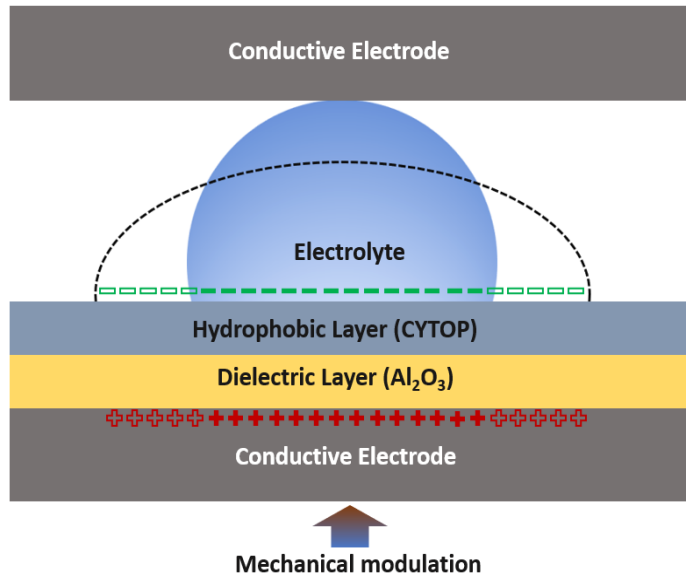

FIGURE 1. REWOD configuration used for this study. Mechanical force applied to either the bottom or top electrodes squeezes the electrolyte, periodically increasing and decreasing the effective interfacial area and generating alternating current

coated with a metal layer for conduction and then with a dielectric layer (e.g. Al_2O_3) with an additional layer of fluoropolymer (e.g. CYTOP) for surface hydrophobicity. An electrolyte is sandwiched between the electrodes which upon oscillation generates AC current due to a modulating electrical capacitance and thus an AC voltage across the electrodes. The formation of electrical capacitance is due to the capacitance from both the electrical double layer (EDL) at the solid-liquid interface and the dielectric insulator [10]. The total capacitance can be modeled as: $C = \varepsilon_0 \varepsilon_r A/d$ where $\varepsilon_0 = 8.85 \times 10^{-12}$ F/m is the vacuum permittivity, ε_r is the relative permittivity of the dielectric material, A is the electrode-electrolyte interfacial area, and d is the thickness of the dielectric layer. Two possible ways the capacitance can be increased are by decreasing the dielectric thickness or by using dielectric materials with high ε_r. However, many high ε_r materials have high thermal instability and resistivity. Dielectric materials such as Al_2O_3 are considered ideal for REWOD applications [11].

One of the performance parameters of REWOD energy harvester is the power density, which is the power generated per unit area (W/cm^2). Power density is one of the most important parameters to consider in energy harvester design because wearable sensors have become significantly miniaturized over the years. There are two pathways to higher power density REWOD energy harvester output. One is the application of bias voltage in which an externally applied voltage induces high current and therefore results in high power density. However, the concept of "self-powered" is significantly compromised in that scenario since the application of an external voltage source would no longer make the device self-powered. On the other hand, much lower power density is achieved without applying any external bias voltage, but the power would not be sufficient to power wearable sensors. Therefore, the small input voltage from the REWOD could be rectified to convert the AC signal to a DC voltage and then boosted and regulated to supply a constant DC power by using a DC-DC converter. All of these components could be integrated within the same device and hence power the device without requiring an external voltage source. The schematic in Figure 2 shows the input AC voltage from the REWOD fed into the rectifier and voltage regulator to rectify and regulate the DC power supply to the motion sensor. Eventually implementing the REWOD electrodes on a flexible and biocompatible material will allow the motion tracking device to be worn on the ankle, thus harvesting energy from regular physical activities. The figure also depicts the REWOD harvester functioning as a motion tracking sensor, where the charge amplifier amplifies the generated charge from the motion activity. Typically, the generated AC voltage amplitude from the REWOD lies in the mV range, lacking the capability of distinguishing motion at various frequencies and displacements due to low resolution. Amplifying the low amount of charge allows to achieve improved signal-to-noise ratio (SNR) as well as high dynamic range for the motion sensor. Having the charge amplifier thus ensures an overall better resolution for the self-powered motion sensor. An analog-to-digital converter (ADC)
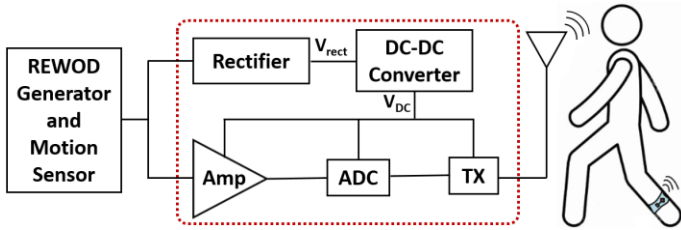
FIGURE 2. The block-level diagram of REWOD based self-powered motion sensor integrated with charge amplifier and DC-DC converter

digitizes the amplified signal and finally a transmitter (TX) transmits the data wirelessly to a remote receiver, which is the eventual goal of this research.

Different architectures and design methods have been used in the past to rectify a low input signal to a higher output power. A self-calibrating energy harvester was developed by Stoopman *et al.* that generated 1 V input signal at -26.3 dBm input power that corresponds to 141 mV_{P-P} input voltage [12]. Similarly, Yi *et al*. designed and implemented a diode connected transistor-based rectifier circuit to rectify a low input signal of 200 mV [13]. However, the prior architectures worked only at MHz frequency range. As the AC signal harvested from the REWOD is fairly low in frequency and amplitude, an efficient low frequency signal (<10 Hz) rectifying circuitry is required to convert the AC signal to DC signal. The AC voltage from the REWOD generated during electrode modulation due to motion activity is fed into a charge amplifier to produce an output voltage proportional to the generated charge [14]. Both the standard commercial-off-the-shelf (COTS) and application-specific integrated circuits (ASIC) approaches for sensor integrated electronics (IE) have been considered in the literature [15-17]. For complicated sensor IEs, e.g. pressure and tactile sensors, the ASIC approach is preferred. Previously reported charge amplifiers used in the transducers are not suitable for low-frequency tracking sensors. For a low-frequency motion detection, a feedback control technique is implemented with the charge amplifier [18]. Feedback path provides good linearity characteristics for low-bandwidth applications. In this paper, the standard COTS-based system is implemented in the motion detection circuitry, which is powered by the REWOD and the associated energy harvesting circuit. The motion sensor will also include the ADC and the TX to wirelessly transmit the motion sensor data to a remote end. This paper focuses on the charge amplifier and the energy harvesting circuit design along with the transducer for the self-powered wearable motion sensor application.

2. EXPERIMENTAL SECTION

2.1 Electrode Fabrication

Two dissimilar electrodes were fabricated using (single-side polished) highly doped P-type silicon wafers with a diameter of 50.5 mm and a thickness of 0.38 mm (University Wafers Inc.). Both wafers were first coated with a ~100-nm-thick titanium

adhesion layer. Before the deposition of dielectric material over the titanium layer, a small portion of the wafer was covered with Kapton tape to block the dielectric insulation and later removed to enable current conduction. A 100-nm-thick dielectric material (Al_2O_3) was deposited on one of the wafers. Both the titanium and dielectric materials were deposited using the NEE-400 dual e-beam evaporator (Nanomaster Inc.). After each deposition, thicknesses were verified using the Alpha-Step D-300 Stylus Profiler (KLA Corporation). After a successful deposition of the desired thickness of the dielectric, an additional layer of hydrophobic fluoropolymer, CYTOP, was deposited. CYTOP (CTL-809M), and its solvent (CT-Solv. 180), both purchased from AGC Chemicals Company, were mixed in a volumetric ratio of 1:3. The solution was spin-coated on the wafer over the dielectric layer using Laurell WS-650MZ. Spin coating was performed at 600 rpm for 5 seconds (spread cycle) and then at 3000 rpm for 50 seconds (spin cycle). The sample was dried at room temperature for 15 minutes, pre-baked for 30 minutes at 80°C, and finally baked again for 60 minutes at 185°C to ensure complete evaporation of the solvent. A complete dielectric electrode sample is illustrated in Figure 3(a) showing the layered electrode structure. An SEM image of the cross-section was obtained using a field-emission scanning electron microscopy (JEOL JSM-7001F), as shown in Figure 3(b) to confirm the thickness and uniformity of different deposited layers.

Approximately 20 mL of 0.5M aqueous solution was prepared using sodium chloride (Sigma Aldrich Inc.) and deionized water and used as an electrolyte. Many REWOD experiments in the past have used electrolytes that are either expensive such as Galinstan or toxic such as mercury. Sodium chloride solution was chosen as a charged form of electrolyte which is not only a convenient form of electrolyte, but also cost effective. However, in practical REWOD application, use of salt solution as an electrolyte would not be feasible.

2.2 Measurement Set-up

The experimental setup for the AC signal (V_{P-P}) generation and measurement is shown in Figure 4. It consisted of an XYZ positioner stage with a long and lightweight acrylic beam attached to it. The beam was used to hold the top electrode stationary. The XYZ positioner was used to set a 4 mm gap between the top and bottom electrodes before the modulation started. Input oscillations were applied using a custom-built subwoofer system that could be controlled with a signal generating app (Audio Function Generator PRO). The shaker system consisted of an 8-inch 800-W subwoofer (Pyle), a 400 W amplifier (Boss CX250), and a 12-V power source (Apevia ATX Raptor) attached to a power adapter cord. This method of producing low-frequency and high-amplitude oscillations has been used in prior published work [19]. A custom wood enclosure provided a location to mount the subwoofer and contained the amplifier and power source. A 3D- printed sample-holding stage was placed over the subwoofer dust cap to provide a flat surface to hold the bottom REWOD substrate. During the electrolyte modulation between the electrodes, generated AC
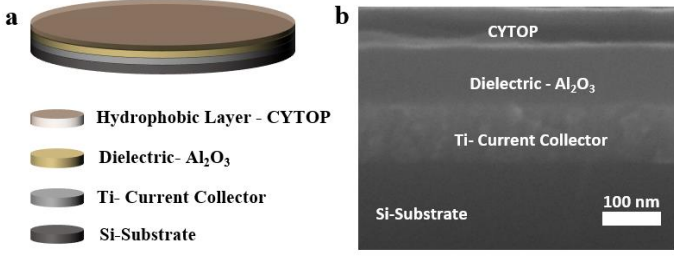
FIGURE 3. (a) Schematic of the dielectric electrode used in REWOD energy harvesting. (b) A cross-sectional view of a fabricated sample obtained by FE-SEM showing individual deposited layers

voltage at various subwoofer oscillation frequencies was measured using an oscilloscope (Keysight InfiniiVision DSOX3014A). The displacement amplitude for each subwoofer frequency was determined by measuring the vertical distance between the electrodes during the modulation using a slow-motion cell phone camera and a ruler. For each frequency step, the amplitude was adjusted in the function generator to replicate the desired displacement.

AC voltage with respect to how much the droplet was squeezed with varying electrode displacements in the vertical direction at 2 Hz frequency was measured using the same set-up as that of varying frequency. The bottom electrode substrate had a constant oscillation of +/-1.25 mm. The initial gap between the top and bottom electrodes ranged from 3.65 mm to 5.25 mm with a step size of 0.2 mm and was precisely controlled using the micrometer scale on the XYZ stage. The resulting droplet deformation percentage in the y-direction, compared to initial gap distance, was 24% to 34%.

2.3 Charge Amplifier

During REWOD operation, charge is generated due to the electrode modulation. This charge was converted to an AC voltage signal and amplified employing charge amplifier (CA)-based IEs [16]. Any human physical activity producing charge can be transmitted wirelessly after the conversion of the charge to a voltage signal and amplification. As was previously mentioned, though ASIC-based IEs are proposed in the literature, this paper presents the standard COTS-based charge amplifier to assess the generated charge from the REWOD. As shown in Figure 5, the prototype includes INA126 amplifier from Texas Instruments as the charge amplifier with a variable gain range of 5 to 10,000 V/V [20]. The amplifier achieves a low noise of 35 nV/√Hz, while consuming 67.5 nW of power. The CA converts the generated charge through an input capacitor, C_{in}, and produces an output voltage, V_{out} at the output node of the amplifier. V_{out} is directly proportional to the generated current of the REWOD. V_{out} can be obtained from the feedback capacitor, C_f and the modulation frequency, f of the electrode displacement using the following equation [21].
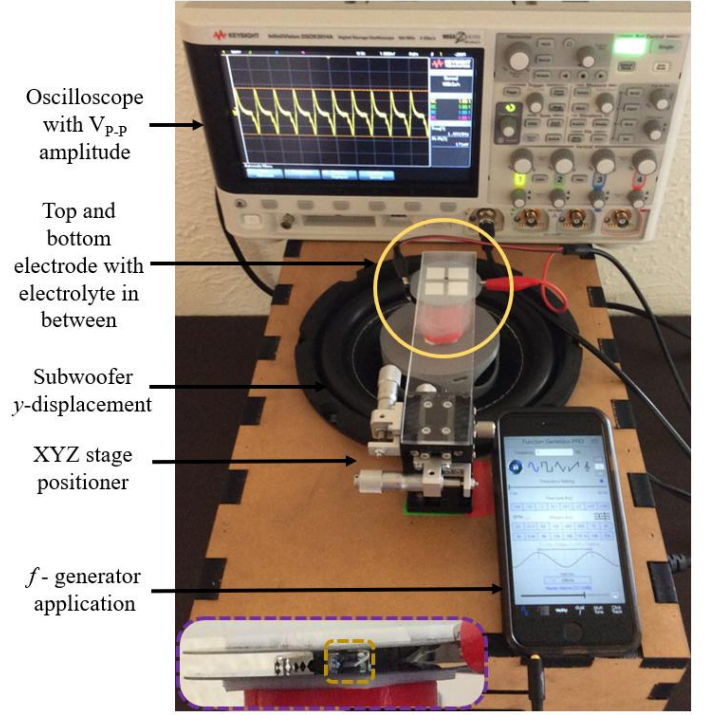

FIGURE 4. REWOD measurement setup illustrating V_{P-P} generation at 1 Hz frequency. The inset shows an electrolyte droplet within the gold dashed line being squeezed between top and bottom electrode substrates

$$V_{out} = \frac{I_{REWOD}}{f C_f} \tag{1}$$

Where I_{REWOD} is the generated current from the REWOD. The amplifier gain was set by the feedback resistor, R_f. A load capacitor was also connected to the output node in order to replicate the input capacitance of the next stage of the system that could either be a low-pass filter or an ADC. The input capacitance (C_{in}) was chosen to be 12 nF to eliminate any DC components from the input AC signal. The gain resistor value (R_f) was chosen to be 4.7 kΩ, to set the CA gain as 24 V/V.
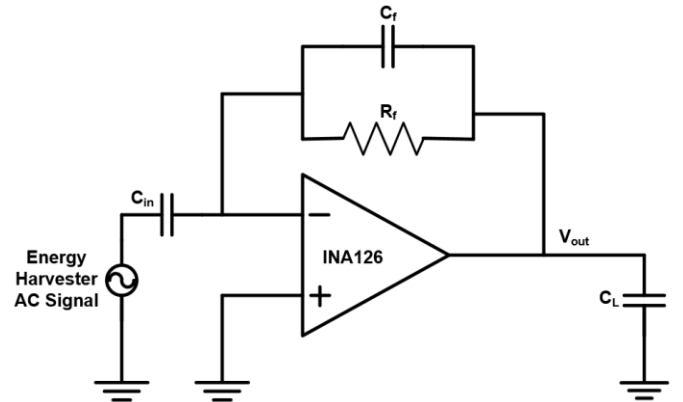

FIGURE 5. Schematic of the charge amplifier

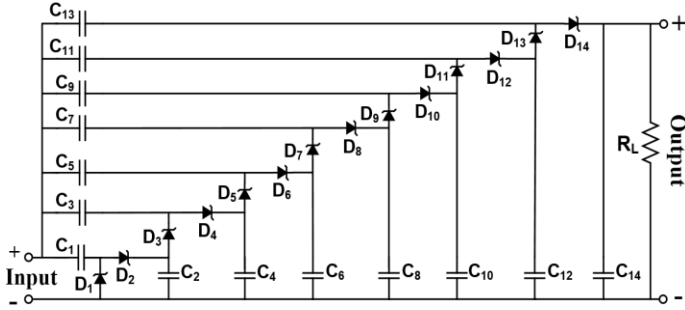## 2.4 Energy Harvester

2.4.1 Rectifier

FIGURE 6. Schematic of a 7-stage voltage-boosting rectifier

The proposed rectifier circuit is a seven-stage voltage-doubler boosting rectifier circuit as shown in Figure 6 to achieve an output voltage of seven times the input voltage [22]. It was designed using SMS7630 Schottky diodes due to the low forward-bias voltage of the Schottky diode architecture. A single-stage voltage-doubler circuit diagram of the 7-stage rectifier circuit consists of two diodes D_1, D_2 and two capacitors C_1 and C_2 as shown in the figure [16]. The architecture works as a full-wave rectifier where D_1 operates during the positive half-cycle and D_2 operates during the negative half-cycle of the input AC signal. To reduce the ripple in the rectified output voltage of the rectifier, the capacitor values were chosen in such a way that the time constant was much larger than the period of the input signal as shown in equations (2) and (3).

$$\frac{I_{rect}}{2\pi C V_{rect}} \ll f \tag{2}$$

$$R_L C \gg T \tag{3}$$

Where I_{rect} and V_{rect} are the output current and voltage of the rectifier, respectively, f is the frequency of the input voltage, R_L is the load resistance, C is the output capacitance, and T is the time period of the input signal. The input and output capacitor values (C_1-C_{14}) were chosen to be 10 µF to produce a smoother DC signal at the output where the desired output current and voltage were 4 mA and 700 mV, respectively. The desired current values were chosen because of the current requirements of the DC-DC converter which is within 2-3 mA. As the DC-DC converter used in this work had a minimum threshold voltage of 700 mV, the minimum desired output voltage from the rectifier was chosen to be 700 mV. The proposed seven-stage voltage boosting rectifier circuit was designed such that it can rectify as low as 70 mV$_{P-P}$ input voltage. To design the rectifier, the SMS7630 Schottky diode by Skyworks with the minimum forward voltage of 135 mV for 1 mA forward current was used.

2.4.2 DC-DC Converter

A COTS component, TPS61220 boost converter by Texas Instruments was used as the voltage regulator in this work [23]. Figure 7 shows the DC boosting circuitry along with the internal circuit of the TPS61220 boost converter. The TPS61220 is a
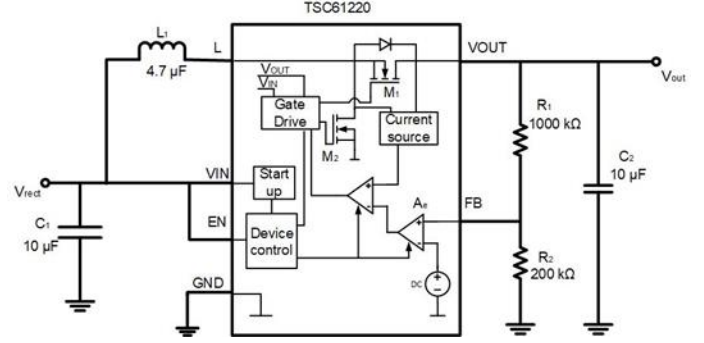

FIGURE 7. Circuit diagram of the TPS61220 DC-DC boost converter

highly efficient switching boost converter. To achieve high efficiency, a synchronous boost topology was used as the power stage. For the power switching, two actively controlled MOSFETs, M_1 and M_2 having low on-resistance were implemented. The input of the TPS61220 boost converter receives varying DC voltages from the rectifier and provides a constant DC voltage at the output. The output DC voltage of the boost converter depends on the external resistor divider (R_1 and R_2) which would vary depending on the application requirements. The input capacitor (C_1 in Figure 7) helps eliminate the fluctuations in the input voltage of the regulator to assist with the transient behavior. The output voltage, V_{out} was regulated using a hysteretic current mode controller which keeps the inductor's (L_1) current constant at 200 mA. A feedback loop and an external reference voltage source were connected to a voltage error amplifier (A_e) to drive the inductor current higher by increasing the voltage across the inductor. During steady-state operation, the inductor's current charges the output capacitor (C_2 in Figure 7) and flows into the load.

3. RESULTS AND DISCUSSION

As there was no bias voltage applied to the REWOD energy harvester during the experiment, the AC voltage generated within the REWOD due to the modulation of the electrolyte between the electrodes was in the range of a few hundreds of millivolts for the frequency range of 1-3 Hz. Figure 8 shows a linear fit AC voltage plotted with respect to increasing frequency. AC peak-to-peak voltage increases linearly with increasing frequency between 1 to 3 Hz with an average slope of ~75 mV/Hz.

As the current increases linearly with increasing frequency, so does the voltage, which satisfies Ohm's law considering resistance remains constant. The AC voltage per unit area (V_{P-P}/cm^2), was determined based on the maximum electrode-electrolyte interfacial area during modulation for a 50 µL electrolyte droplet and 2.5 mm displacement, which was previously calculated to be 0.3 cm^2. Thus, the AC peak-to-peak voltage density (V_{P-P}/cm^2) was found to be in the range of 0.32-0.8 V_{P-P}/cm^2 for this work. The voltage generated across the REWOD electrodes is the result of a continuous change in capacitance and hence an alternating current along with the
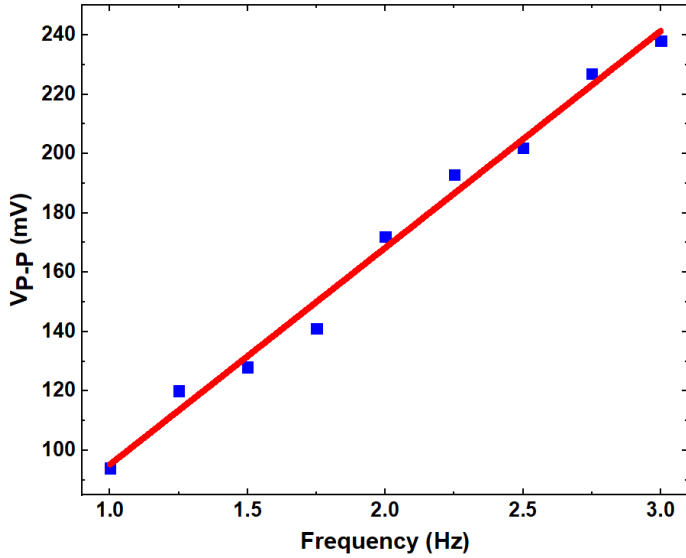
FIGURE 8. AC voltage output (linear fit) from the REWOD with respect to the frequency (1 Hz to 3 Hz with 0.25 Hz step)

effective system resistance arising from the conductive layer, dielectric layers (Al_2O_3 and CYTOP), and electrolyte.

With the increasing electrode-electrolyte interfacial area, AC current increases resulting in an increase of AC voltage. Interestingly, the increase in AC voltage with increasing displacement was not as linear as with the increasing frequency, rather almost parabolic. This is because the electrode-electrolyte interfacial area is circular in geometry since the electrolyte is sandwiched between the electrodes. As the circular contact area increases with increasing droplet deformation ($A = \pi r^2$), the AC voltage increases almost parabolically. Figure 9 shows such parabolic relation of increasing AC voltage with respect to the increasing droplet deformation at a fixed oscillation frequency of 2 Hz. From a 50 µL volume of electrolyte for the droplet deformation percentage between 24-34 %, AC voltage was in the range of 71 mV_{P-P} to 422 mV_{P-P}. In terms of AC voltage per unit area (V_{P-P}/cm^2), the voltage density ranged from 0.39 V_{P-P}/cm^2 to 0.97 V_{P-P}/cm^2 for the given displacements. The range of AC voltage from the REWOD is significant given the fact that it completely arose within the electrode-electrolyte interface without any external voltage source.

The generated AC voltage signal from the REWOD was also applied to the charge amplifier in order to produce an amplified output voltage while varying both the frequency and the droplet deformation. An amplified voltage over varying frequency band from 1 Hz to 3 Hz was determined to be between 2.3 V_{P-P} to 5.8 V_{P-P}. The amplified output voltage proportionally corresponded with the measured AC voltage output from the REWOD in terms of linearity. The amplified peak-to-peak voltage output with respect to varying frequency is shown in Figure 10. Likewise, the amplified peak-to-peak voltage over the droplet deformation range of 24-34% is presented in Figure 11. With the increasing displacement, the amplified voltage increased over the range, but didn't follow a linear trend, rather
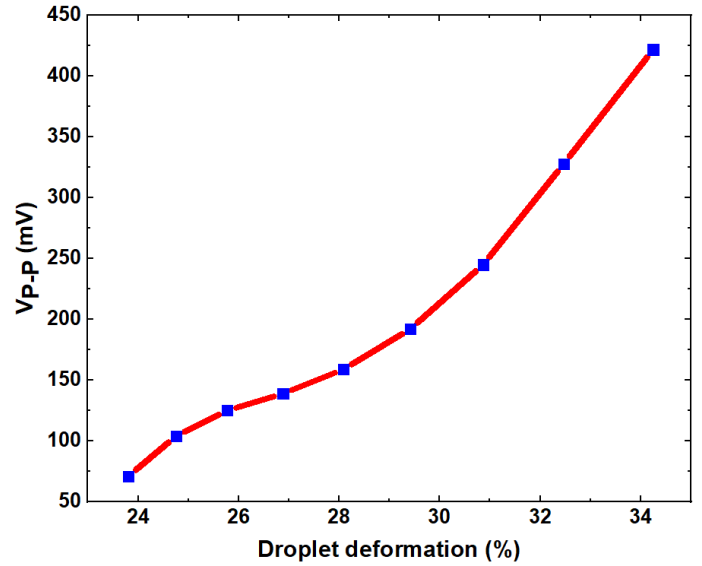

FIGURE 9. AC voltage output from REWOD with respect to droplet deformation (24% to 34%) at 2 Hz oscillation frequency

increased parabolically agreeing with the increasing trend of REWOD output voltage with increasing displacement. In order to pass all the current through the feedback path of the CA, the feedback capacitor (C_f) was chosen to be 500 pF.

The AC signal harvested by the REWOD was rectified using the proposed rectifier. As the frequencies of interest were within the range of 1 to 3 Hz, the corresponding rectified voltage output is shown in Figure 12. The minimum harvested AC signal was 94 mV_{P-P} for the minimum 1 Hz frequency for which the output rectified voltage was found to be 63 mV DC. Figure 12 shows the simulated and measured output DC voltage of the rectifier for different frequencies with step size of 0.25 Hz. The maximum measured output voltage was 963 mV for the input AC voltage
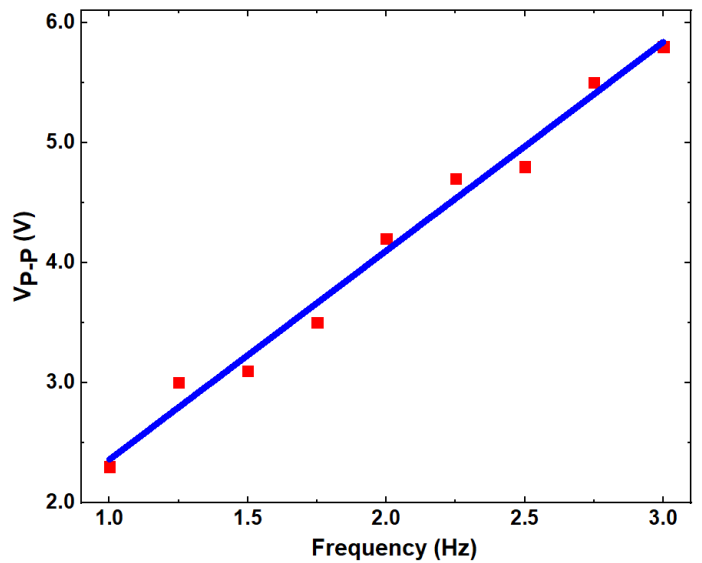

FIGURE 10. Amplified AC voltage output (linear fit) from the charge amplifier with respect to frequency (1 Hz to 3 Hz with 0.25 Hz step)
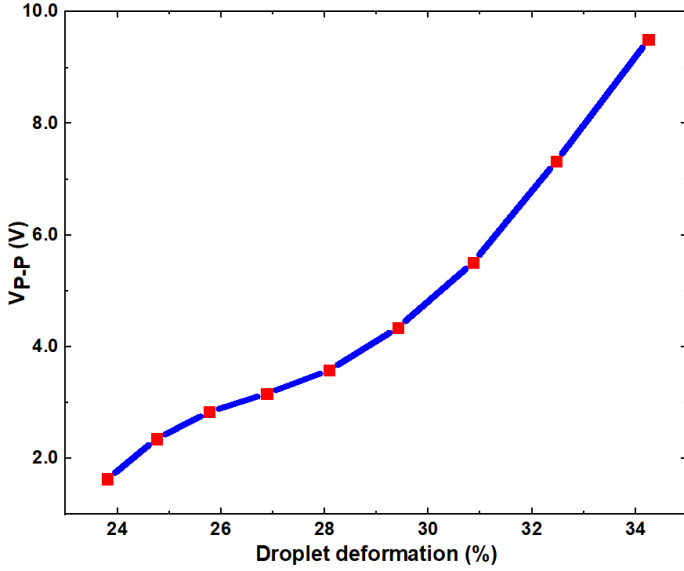
FIGURE 11. Amplified AC voltage output from the charge amplifier with respect to droplet deformation (24% to 34%) at 2 Hz of oscillation frequency
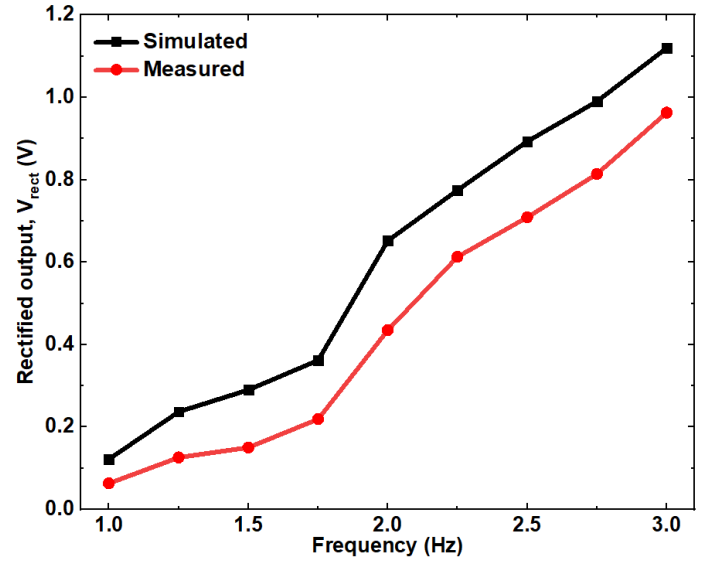

FIGURE 12. Simulated (black line) and measured (red line) rectifier output voltage with respect to frequency for output AC voltage from REWOD

signal of 238 mV$_{P-P}$ at 3 Hz frequency. The simulation of the rectifier was performed using LTspice software. The diode SMS7630 was created in LTspice by modifying the forward voltage and forward current according to the data sheet. The simulation results show higher voltage outputs compared to the measured voltages. This is due to the fact that the simulation uses the lossless ideal components to run the simulation. Figure 13 shows the rectified output voltage for the harvested AC voltage from the REWOD energy harvester due to varying droplet deformations. The minimum harvested voltage at 24 % droplet deformation was 71 mVp-p for which the measured rectified DC voltage was 98 mV at 2 Hz frequency. A maximum DC voltage of 1.39 V was measured at 34% droplet deformation.

The commercially available DC-DC converter model was simulated using LTSpice software as well. The voltage range of the TPS61220 boost converter was 0.7 to 5 V, which requires the minimum DC voltage output from the rectifier to be 0.7 V. The measured voltage output of the boost converter is shown in Figure 14 where 1 MΩ load resistor was used. It can be seen from the figure that the output voltage of the boost converter, V_{out} was a constant 3 V when the V_{rect} was within 0.7 V to 3.3 V range. Above 3.3 V, V_{out} increased slightly to 3.3 V. The minimum input voltage required for the DC-DC converter was achieved when the rectifier input voltage was 200 mV$_{P-P}$. As shown earlier in Figure 11, for the input voltage of 200 mV$_{P-P}$, the rectifier could provide above 700 mV output for all three oscillation frequencies. The DC-DC converter is able to generate 9 μW of DC power for an output load of 1 MΩ. To put it into perspective, the DC output power scales up to 30 μW/cm^2 in terms of power density, which is significant considering the volume of electrolyte used (50 μL) and 2.5 mm of electrode displacement.

Finally, a summary of REWOD AC voltage with respect to frequency and electrolyte droplet deformation along with their corresponding output voltage are presented in Table 1 and 2. Even though both the rectified and boosted output voltage include measured as well as simulated results, REWOD output AC voltage and amplified voltage include only the measured results. In order to have a meaningful comparison among input and output voltages, the summary tables include only the measured results. Table 1 summarizes the input AC voltage with varying frequencies and their corresponding voltage; amplified, rectified, and boosted. Similarly, Table 2 summarizes the input
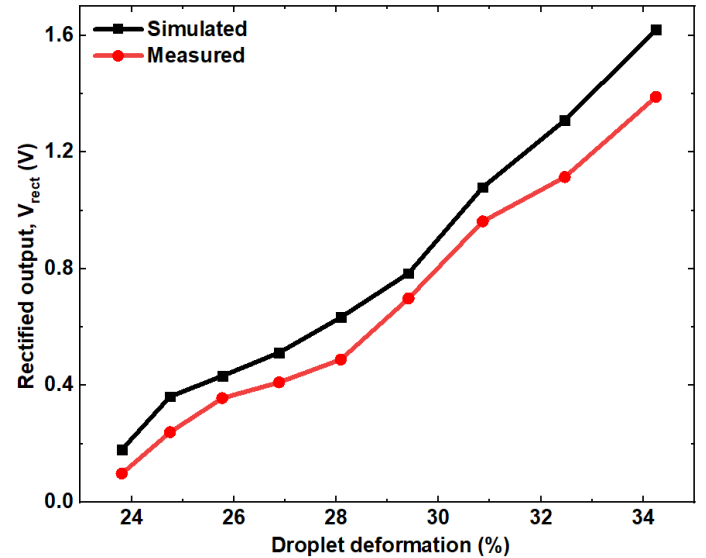

FIGURE 13. Simulated (black line) and measured (red line) rectifier output voltage at 2 Hz frequency with respect to droplet deformation (24% to 34%) for output AC voltage from REWOD
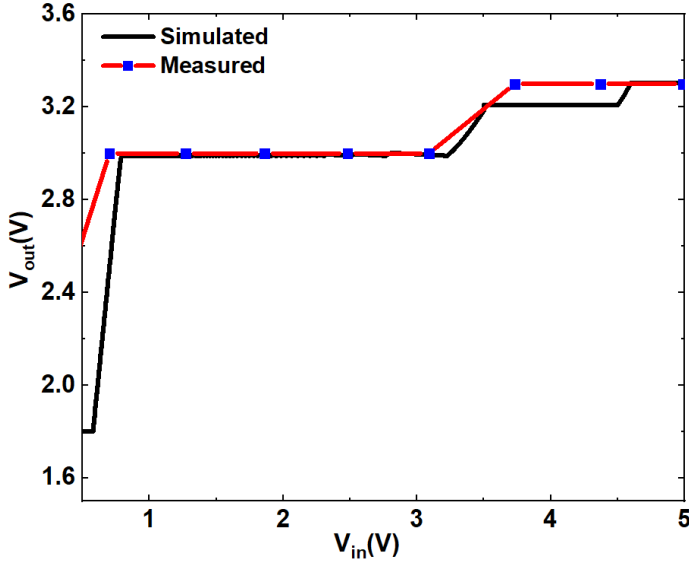
FIGURE 14. Simulated (black line) and measured (red line) output voltage of the boost converter

TABLE 1. Summary of input and output voltages with frequencies

Frequency (Hz)	V_{in} (mV)	V_{amp} (V)	V_{rect} (V)	V_{boost} (V)
1.00	94	2.30	0.06	1.01
1.25	120	3.00	0.13	1.52
1.50	128	3.10	0.15	1.61
1.75	141	3.50	0.22	1.73
2.00	172	4.20	0.44	2.55
2.25	193	4.70	0.61	2.65
2.50	202	4.80	0.71	3.00
2.75	227	5.50	0.81	3.00
3.00	238	5.80	0.96	3.00

TABLE 2. Summary of input and output voltages with respect to electrolyte droplet deformation (%)

Droplet deformation (%)	V_{in} (mV)	V_{amp} (V)	V_{rect} (V)	V_{boost} (V)
24	71	1.63	0.10	1.12
25	104	2.35	0.24	1.75
26	125	2.83	0.36	2.10
27	139	3.16	0.41	2.48
28	159	3.58	0.49	2.63
29	192	4.34	0.70	3.00
31	245	5.51	0.96	3.00
32	328	7.32	1.12	3.00
34	422	9.5	1.39	3.00

AC voltage with varying electrolyte droplet deformation and their corresponding voltages; amplified, rectified, and boosted.

4. CONCLUSION

In this work, REWOD based mechanical motion energy harvesting was implemented without requiring any external bias voltage. AC voltage across the electrodes due to AC current generation with continuous charging and discharging of the electrodes was measured with respect to varying frequency and electrode displacements. The AC voltage from the REWOD with respect to frequency (1 - 3 Hz) for 2.5 mm displacement was in the range of ~95-240 mV for a 50 µL droplet of electrolyte. Similarly, the AC voltage from the REWOD with respect to droplet deformation from 24% to 34% due to varying electrode displacements at 2 Hz oscillation frequency was in the range of 71 - 422 mV. This range of frequency and displacement align very well with various human motion activities, but the voltage is too low for practical applications. Therefore, the REWOD AC voltage was converted to a constant DC power source using a multistage rectifier, and a DC-DC boost converter. Likewise, the rectified DC voltage of 0.7 V provided a constant 3 V of output voltage through the boost DC-DC converter signifying that the REWOD energy harvester with integrated charge amplifier and boost converters can be used as a self-powered motion sensor. In the future, a single unit device that comprises the REWOD energy harvester and the components for power conditioning and amplification could be integrated together and worn on an arm, an ankle, or a knee, etc. for motion sensing to detect whether a person is at rest, walking, or running as part of human health monitoring in real time.

REFERENCES

[1] D. Dias and J. Paulo Silva Cunha, "Wearable Health Devices-Vital Sign Monitoring, Systems, and Technologies," *Sensors (Basel)*, vol. 18, no. 8, Jul. 2018.

[2] D. Larcher and J.-M. Tarascon, "Towards greener and more sustainable batteries for electrical energy storage," *Nat Chem*, vol. 7, no. 1, pp. 19-29, Jan. 2015.

[3] D.-A. Wang and K.-H. Chang, "Electromagnetic energy harvesting from flow induced vibration," *Microelectronics Journal*, vol. 41, no. 6, pp. 356-364, Jun. 2010.

[4] Taeho Oh, S. K. Islam, G. To, and M. Mahfouz, "A low-power CMOS energy harvesting circuit for wearable sensors using piezoelectric transducers," in *2017 United*

States National Committee of URSI National Radio Science Meeting (USNC-URSI NRSM), Jan. 2017, pp. 1-2.

[5] B.-Y. Lee, D. H. Kim, J. Park, K.-I. Park, K. J. Lee, and C. K. Jeong, "Modulation of surface physics and chemistry in triboelectric energy harvesting technologies," *Sci Technol Adv Mater*, vol. 20, no. 1, pp. 758-773, Jun. 2019.

[6] F. U. Khan and M. U. Qadir, "State-of-the-art in vibration-based electrostatic energy harvesting," *Journal of Micromechanics and Microengineering*, vol. 26, no. 10, p. 103001, Oct. 2016.

[7] B. Meng *et al.*, "A high performance triboelectric generator for harvesting low frequency ambient vibration energy," in *2014 IEEE 27th International Conference on Micro Electro Mechanical Systems (MEMS)*, Jan. 2014, pp. 346-349.

[8] T. Krupenkin and J. A. Taylor, "Reverse electrowetting as a new approach to high-power energy harvesting," *Nature Communications*, vol. 2, p. 448, Aug. 2011.

[9] P. Garcí-Sánchez and F. Mugele, "Fundamentals of Electrowetting and Applications in Microsystems," in *Electrokinetics and Electrohydrodynamics in Microsystems*, A. Ramos, Ed. Vienna: Springer, 2011, pp. 85-125.

[10] R. Parsons, "The electrical double layer at solid/liquid interfaces," *Journal of Electroanalytical Chemistry and Interfacial Electrochemistry*, vol. 118, pp. 3-18, Feb. 1981.

[11] H. Yang, S. Hong, B. Koo, D. Lee, and Y.-B. Kim, "High-performance reverse electrowetting energy harvesting using atomic-layer-deposited dielectric film," *Nano Energy*, vol. 31, pp. 450-455, Jan. 2017.

[12] M. Stoopman, S. Keyrouz, H. J. Visser, K. Philips, and W. A. Serdijn, "A self-calibrating RF energy harvester generating 1V at −26.3 dBm," in *2013 Symposium on VLSI Circuits*, Jun. 2013, pp. C226-C227.

[13] J. Yi, W.-H. Ki, and C.-Y. Tsui, "Analysis and Design Strategy of UHF Micro-Power CMOS Rectifiers for Micro-Sensor and RFID Applications," *IEEE Transactions on Circuits and Systems I: Regular Papers*, vol. 54, no. 1, pp. 153-166, Jan. 2007.

[14] L. Pinna and M. Valle, "Charge amplifier Design Methodology for PVDF-Based Tactile Sensors," *Journal of Circuits, Systems, and Computers*, 2013.

[15] F. Wohlstreicher, "Charge amplifier for sensors outputting electrical charge," US5371472A, Dec. 06, 1994.

[16] T. Koivistoinen, S. Junnila, A. Värri, and T. Kööbi, "A new method for measuring the ballistocardiogram using EMFi sensors in a normal chair," *Conf Proc IEEE Eng Med Biol Soc*, vol. 2004, pp. 2026-2029, 2004.

[17] S. Mizuno, K. Fujita, H. Yamamoto, N. Mukozaka, and H. Toyoda, "A 256×256 compact CMOS image sensor with on-chip motion detection function," *IEEE Journal of Solid-State Circuits*, vol. 38, no. 6, pp. 1072-1075, Jun. 2003.

[18] A. J. Fleming and S. O. R. Moheimani, "A grounded-load charge amplifier for reducing hysteresis in piezoelectric tube scanners," *Review of Scientific Instruments*, vol. 76, no. 7, p. 073707, Jun. 2005.

[19] T. Perera, S. A. C. Yohanandan, and H. J. McDermott, "A simple and inexpensive test-rig for evaluating the performance of motion sensors used in movement disorders research," *Med Biol Eng Comput*, vol. 54, no. 2-3, pp. 333-339, Mar. 2016.

[20] Texas Instrument Datasheet, "INA126 d Micro-Power Instrumentation Amplifier Single and Dual Versions.

[21] I. Mahbub *et al.*, "A Low-Power Wireless Piezoelectric Sensor-Based Respiration Monitoring System Realized in CMOS Process," *IEEE Sensors Journal*, vol. 17, no. 6, pp. 1858-1864, Mar. 2017.

[22] N. T. Tasneem, S. R. Suri, and I. Mahbub, "A low-power CMOS voltage boosting rectifier for wireless power transfer applications," in *2018 Texas Symposium on Wireless and Microwave Circuits and Systems (WMCS)*, Apr. 2018, pp. 1-4.

[23] Texas Instrument Datasheet, "TPS61220 Low Input Voltage, 0.7V Boost Converter with 5.5μA Quiescent Current.